Journal of Applied Phycology
https://doi.org/10.1007/s10811-022-02724-z

Chlorophyta microalgae as dietary protein supplement: a comparative analysis of productivity related to photosynthesis

Costanza Baldisserotto[1] · Alessandra Sabia[1] · Martina Giovanardi[1] · Lorenzo Ferroni[1] · Michele Maglie[2] · Simonetta Pancaldi[1]

Received: 22 October 2021 / Revised and accepted: 5 March 2022

Abstract
Microalgae are studied as innovative sources of a wide range of highly valuable products, including proteins for the food/feed sectors. However, protein content varies depending on algal species, culture conditions and harvesting period. The Phylum Chlorophyta includes most of the described species of green algae. Due to their remarkable peculiarities, four Chlorophyta species belonging to two distinct classes were selected for the research: *Chlorella vulgaris* and *Chlorella protothecoides* as Trebouxiophyceae, and *Neochloris oleoabundans* and *Scenedesmus acutus* as Chlorophyceae. The algae were studied to obtain comparative results about their growth performance, and total protein content and profile under the same culture conditions. Since photosynthetic process directly influences biomass production, photosynthetic pigment, PSII maximum quantum yield and thylakoid protein content and profile were analysed. SDS-PAGE and 2D BN/SDS-PAGE were performed to expand information on the organization and assembly of the resolved thylakoid complexes of samples. Despite the algal species showed similar growth rates and photosynthetic efficiency, *S. acutus* showed the highest capability to accumulate proteins and photosynthetic pigments. Regarding the thylakoid protein profile, the two Trebouxiophyceae showed very similar pattern, whereas different amounts of LHCII occurred within the two Chlorophyceae. Finally, the separation of thylakoid protein complexes in 2D BN/SDS-PAGE revealed a more complex pattern in *S. acutus* as compared to the other species. Overall, it is suggested that a higher stability of the photosynthetic membranes can result in higher biomass and protein production. Altogether, results have highlighted the metabolic uniqueness of each strain, resulting in a non-obvious comparison with the other species.

Keywords Blue Native PAGE · Chlorophyta · Microalgae · Photosynthetic performance · Protein content · Thylakoid protein complexes

Introduction

The potential of microalgae as a source of renewable energy and high-value bio-products has been widely explored (Khan et al. 2018; Camacho et al. 2019). For nutritional purposes, proteins and lipids, especially omega-3 polyunsaturated fatty acids (PUFAs), are the most interesting molecules; moreover, vitamins, oxidation-protecting pigments (i.e. carotenoids, Cars) and other compounds contribute to the nutritional value of microalgae (Hayes et al. 2017; Wells et al. 2017; Khan et al. 2018; Camacho et al. 2019; Parisi et al. 2020). The advantage of cultivating these organisms on non-arable land, extreme environments up to space, in microgravity conditions (Stankovic 2018), lets us consider them a "crop for the future" (Torres-Tiji et al. 2020). Among the aforementioned compounds, proteins are one of the most important and can represent up to 50% of the total microalgal biomass dry weight (DW) (Lourenço et al. 2004; Hayes et al. 2017; Camacho et al. 2019). Moreover, various microalgal species are studied as innovative sources of proteins in food sectors, not only for their high protein

Costanza Baldisserotto and Alessandra Sabia contributed equally to this work.

✉ Simonetta Pancaldi
simonetta.pancaldi@unife.it

[1] Department of Environmental and Prevention Sciences, University of Ferrara, C.so Ercole I d'Este, 32, 44121 Ferrara, Italy

[2] Department of Life Sciences and Biotechnology, University of Ferrara, C.so Ercole I d'Este, 32, 44121 Ferrara, Italy

Published online: 02 May 2022

content, but also for the nutritional quality, which is comparable to that of other referenced food proteins (Spolaore et al. 2006; Hayes et al. 2017; Khan et al. 2018; Jayappriyan et al. 2021). Among the protein-rich microalgae, *Chlorella* and *Arthrospira* are the most widely used both as food and as a nutraceutical supplement. The success of these algae for the market is linked to their high content in different types of proteins, some of which positively impact health, for example by reducing cholesterol levels (Hayes et al. 2017; Khan et al. 2018). However, other microalgae species, like those belonging to *Scenedesmus*, *Dunaliella* and *Aphanizomenon* genera, are proposed to produce proteins with nutraceutical potential (Buono et al. 2014). In this perspective and taking into account the increasing protein demand for nutrition (Henchion et al. 2017; FAO 2020), the identification of the best microalgal strains is a current and challenging issue. It is well known that protein content and pattern in microalgae are highly influenced by culture conditions, growth phases and morphological and structural characteristics of each species (Meijer and Wijffels, 1998; Lourenço et al. 2004; Tran et al. 2009; Laurens et al. 2014). Consequently, a direct comparison of protein content in different microalgae is very difficult. Furthermore, several methods are employed for protein extraction and quantification; thus, especially when comparing data from literature, this makes the comparison between species even more complex (Meijer and Wijffels, 1998; Barbarino and Lourenço 2005; Ursu et al. 2014).

Taking these issues into account, this study analyses the protein content and pattern of four microalgae species belonging to the same Phylum (Chlorophyta) and cultivated under identical culture conditions. Chlorophyta include most of the described species of green algae which are characterised by great morphological diversity and by the ability to grow in a wide range of environmental conditions (Leliaert et al. 2012). Due to these remarkable peculiarities and on the basis of their phylogenetic position, four Chlorophyta species were selected: *Chlorella vulgaris* and *Chlorella protothecoides* (both Trebouxiophyceae), and *Neochloris oleoabundans* and *Scenedesmus acutus* (both Chlorophyceae) (Fig. 1). Although a 2-to-2 comparison based on four species cannot provide totally comprehensive information, it is nevertheless useful for improving knowledge about Chlorophyta and highlights possible differences between the two classes with the highest biotechnological potential, Trebouxiophyceae and Chlorophyceae (Garrido-Cardenas et al. 2018). Modern molecular studies state that algae belonging to these two classes, even if share similar morphological shape, are characterised by a remarkable diversity of physiological and biochemical constraints, since they have evolved in independent phylogenetic lineages because of convergent evolution within Chlorophyta (Fang et al. 2017). Among the Trebouxiophyceae, *C. vulgaris* is one of the best-studied microalgae and is considered a model organism in plant science (Krienitz et al. 2015). Due to its high adaptability to a variety of environmental conditions and high productivity in large-scale cultivation systems, this strain is widely exploited for several biotechnological applications including food, feed, cosmetics and pharmaceuticals production, wastewater treatments or as renewable energy source (Khan et al. 2018; Camacho et al. 2019). Moreover, the European Food Safety Authority (EFSA) considers *C. vulgaris* a functional safe food due to its high protein, vitamin and mineral content (Chacón-Lee and González-Mariño, 2010). *Chlorella protothecoides* (now named *Auxenochlorella protothecoides*) has been chosen due to its capability to produce large quantities of lipids, suitable for biodiesel production, and PUFAs, employed in the food industry as supplements (Heredia-Arroyo et al. 2010; Patel et al. 2018). Moreover, based on the availability of its genome, this species could become a model oleaginous microalga, also suitable for the application of genetic engineering tools (Gao et al. 2014; Wu et al. 2015). Among Chlorophyceae, *Neochloris oleoabundans* (now named *Ettlia oleoabundans*) is an attractive candidate for biodiesel production because of its high capability

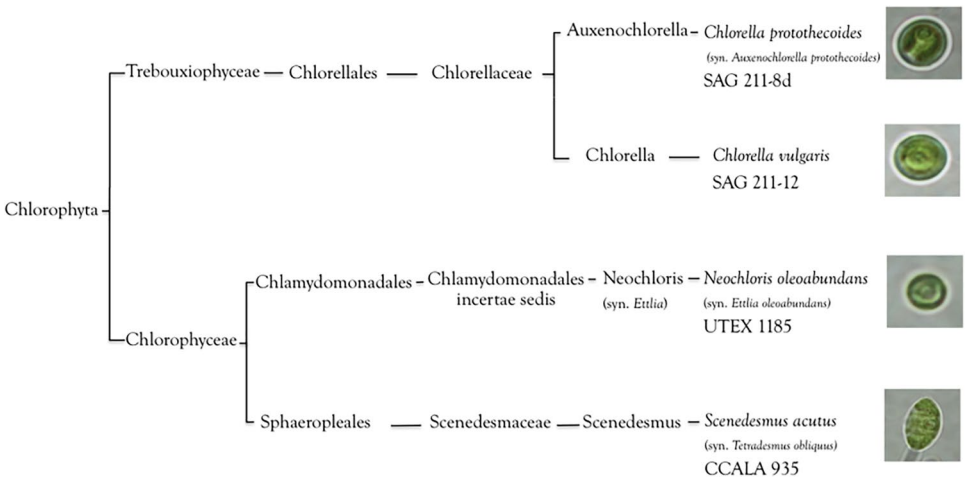

Fig. 1 The phylogenetic position of the four selected Chlorophyta species: two Trebouxiophyceae (*Chlorella protothecoides* and *Chlorella vulgaris*) and two Chlorophyceae (*Neochloris oleoabundans* and *Scenedesmus acutus*)

to accumulate lipids under stress or mixotrophic conditions (Pruvost et al. 2009; Baldisserotto et al. 2016). Moreover, the bioactivity of extracellular polysaccharides released by this alga has been recently ascertained (Li et al. 2020). Finally, the green alga *Scenedesmus acutus* (now named *Tetradesmus obliquus*) was selected for its ability to produce large amounts of proteins and it is considered a good candidate to be source of essential and non-essential amino acids (da Silva et al. 2020). Besides, *S. acutus* is used as a model organism to produce lipids for biodiesel and other industrially important co-products, such as β-carotene, omega-3 fatty acids, glycerol and bioethanol (Damiani et al. 2014; Patnaik and Mallick 2015). Overall, there are many publications on lipid production by the four Chlorophyta listed above, while relatively less information is available on their content of proteins, especially in relation to photosynthetic proteins (for example, thylakoid proteins) or photosynthesis in general, which supports the primary metabolisms in these unicellular microorganisms.

In the present work, the four selected Chlorophyta species were cultivated at a laboratory scale under identical culture conditions to obtain comparative results on their growth performances and protein content and profile, which could be propaedeutic in view of large-scale cultivations for industry. Furthermore, photosynthetic pigment content, photosystem II (PSII) maximum quantum yield (F_V/F_M ratio) and the organization and assembly of the resolved thylakoid complexes were analysed, since the photosynthetic mechanism, which these parameters provide an indication of, directly influences algae growth and consequently biomass production. For the latter issue, thylakoid proteins were analysed by sodium dodecyl sulphate–polyacrylamide gel electrophoresis (SDS-PAGE) and Blue Native (BN)-PAGE in second dimension (2D BN/SDS-PAGE) electrophoresis. Indeed, research on the organization and assembly of the photosynthetic proteins in thylakoids of green microalgae still needs progress. Studies on this field have mainly concerned the model green alga *Chlamydomonas reinhardtii* (Nama et al. 2015, 2019; Devadsu et al. 2021), while only a few studies have examined other species of green algae, like *S. obliquus*, *Botryococcus braunii* or *N. oleoabundans* under mixotrophic conditions (Kantzilakis et al. 2007; Giovanardi et al. 2017; van den Berg et al. 2020). On the other hand, exhaustive knowledge of the photosynthetic machinery represents a valid tool for a better exploitation of photosynthetic organisms. In this regard, it is supposed that high biomass and protein production by plant organisms, including microalgae, are directly linked to the whole photosynthetic process, also involving aspects on the thylakoid membrane architecture and stability.

Materials and methods

Algal strains and culture condition

Microalgal strains used in this study were selected within two classes of Chlorophyta: Trebouxiophyceae (*Chlorella protothecoides* and *Chlorella vulgaris*) and Chlorophyceae (*Neochloris oleoabundans* and *Scenedesmus acutus*) (Fig. 1). *Chlorella protothecoides* SAG 211-8d (Chlorophyta, Trebouxiophyceae, Chlorellales, Chlorellaceae; currently regarded as a synonym of *Auxenochlorella protothecoides*) and *Chlorella vulgaris* SAG 211–12 (Chlorophyta, Trebouxiophyceae, Chlorellales, Chlorellaceae; type species of the genus *Chlorella*) were obtained from the Culture Collection of Algae at the University of Goettingen (SAG, Germany; www.uni-goettingen.de). *Neochloris oleoabundans* UTEX 1185 (formerly Chlorophyta, Chlorophyceae, Sphaeropleales; currently a synonym of *Ettlia oleoabundans*, Chlorophyceae, Chlamydomonadales, Chlamydomonadales *incertae sedis*) was obtained from the Culture Collection of the University of Texas (UTEX, USA; www.utex.org), while *Scenedesmus acutus* PVUW12 (Chlorophyta, Chlorophyceae, Sphaeropleales, Scenedesmaceae; currently regarded as synonym of *Tetradesmus obliquus* (Turpin) M.J. Wynne) was kindly provided by Prof. Erik Nielsen (Department of Biology and Biotechnology, University of Pavia, Italy). *Scenedesmus acutus* PVUW12 corresponds to *Scenedesmus cf. acutus* Meyen CCALA-935, deposited at the Culture Collection of Autotrophic Organisms from Institute of Botany, Academy of Sciences of the Czech Republic, Centre of Phycology, Dukelská. Classification of the organisms follows updated information available on the Algae Base platform (www.algaebase.org).

All microalgae were manipulated axenically using sterilised media, flasks and tools. All algal cultures were inoculated at an optical density (OD_{750}) ranging between 0.03 and 0.04 in 500-mL Erlenmeyer flasks (300 mL of total culture volume) containing BG11 medium (http://www.ccap.ac.uk). All algae were cultivated under same conditions in a KW, model W86RS, growth chamber (24 ± 1 °C temperature, 80 $\mu mol_{photons}\ m^{-2}\ s^{-1}$ PAR provided by cool-white, fluorescent Philips Master TL-D 30 W/840 tubes, 16:8 h of light-darkness photoperiod; KW Apparecchi Scientifici Srl, Italy), with continuous shaking at 80 rpm and without external CO_2 supply.

For morpho-physiological analyses and photosynthetic pigment quantification, aliquots of algae were periodically collected during an 18-day-long growth period. For protein analyses (both total and thylakoid proteins), aliquots

of samples were harvested when the microalgal cultures reached the stationary phase of growth (18th day of cultivation). Experiments were performed at least in triplicate.

Growth evaluations: cell density, optical density and dry biomass

Growth evaluations were carried out on algal samples at different times of cultivation during 18-day-long experiments. Cell density was evaluated using a Thoma haemocytometer (HBG, Giessen, Germany) and plotted on a logarithmic scale to obtain growth kinetics. Cell density was also employed to estimate the specific growth rates during the exponential phase (μ, day^{-1}) (Giovanardi et al. 2013; Baldisserotto et al. 2020). Parallelly, growth of samples was also estimated by measuring the OD_{750}.

For dry biomass determination (DW of algal biomass per litre; g_{DW} L^{-1}), aliquots of samples were filtered through pre-dried and pre-weighed GF/F glass-fibre filters (0.7-μm pore diameter; Whatman). Filters with cell pellets were rinsed with distilled water, dried for 72 h at 60 °C to constant weight and weighed.

During the growth period, total pH of culture media was periodically monitored using a bench pH meter.

Photosynthetic pigment extraction and quantification

For all algae species, extractions of photosynthetic pigments were performed according to Baldisserotto and coworkers (2014) with absolute methanol for 10 min at 80 °C. All manipulations were performed under a dim-green light to avoid photodegradation. Pigment concentrations were evaluated according to equations reported in Wellburn (1994) and expressed on a cell basis ($nmol_{PIG}$ 10^{-6} cells), by counting cells with the Thoma's chamber described above, and/or percentage of algal dry weight (%DW), by dividing pigment content by biomass concentration.

Maximum quantum yield of PSII measurements

In order to determine the in vivo chlorophyll fluorescence of photosystem II (PSII), an ADC OS1-FL Pulse Amplitude Modulated (PAM) fluorometer (ADC Bioscientific Ltd., UK) was used with the following settings: measuring light (ML), 655 nm; saturation pulse (SP), 0.6 s of white light (350–690 nm) at 15,000 $\mu mol_{photons}$ m^{-2} s^{-1}. For the measurements of the maximum yield of PSII, samples were dark-adapted for 15 min and prepared according to that reported in Ferroni et al. (2018). The PSII maximum quantum yield was reported as F_V/F_M ratio, where F_V is the variable fluorescence ($F_M - F_O$), F_M is the maximum fluorescence measured flashing the samples with a saturating light pulse and F_O is the original, basal fluorescence of samples in the dark (Lichtenthaler et al. 2005; Kalaji et al. 2014).

Total protein extraction and quantification

The total protein content was evaluated by extracting two different fractions of soluble proteins: an easily extractable fraction (fraction 1, F1) and a less-easily extractable protein fraction (fraction 2, F2). Fraction 2 contains less soluble proteins, which include also transmembrane proteins. In detail, aliquots of algal samples were centrifuged for 10 min at 500 × *g* and treated according to Baldisserotto et al. (2016) (initial set up based on Ivleva and Golden 2007), with some modifications. Pellets were resuspended in 2 mL of soluble proteins buffer (soluble-PB: 2 mM Na_2EDTA, 5 mM ε-aminocaproic acid, 5 mM $MgCl_2$, 5 mM dithiothreitol dissolved in PBS buffer 1x; PBS buffer (stock solution 10x): 80 g NaCl, 2 g KCl, 14.4 g $Na_2HPO_4 \times 2H_2O$, 2.4 g KH_2PO_4 dissolved in 1L of distilled water), transferred into Eppendorf tubes and then centrifuged (10 min, 2000 × *g*) (washing step). Subsequently, pellets were resuspended in 200 μL of soluble-PB. For three times, samples were frozen in liquid N_2 for 2 min and subsequently heated at 80 °C for other 2 min, then rapidly frozen in liquid N_2 and kept at − 20 °C overnight. The following day, samples were added with glass beads (0.40–0.60-μm diameter; Sartorius, Germany) and vigorously vortexed for 10 min (mixing cycles of 30 s followed by cooling on ice for 30 s). After the addition of 100 μL of soluble-PB, samples were centrifugated (10 min, 1500 × *g*) and the supernatants (F1 fraction with easily extractable, soluble proteins extract) were harvested, rapidly frozen in liquid N_2 and kept at − 20 °C until analyses. The remaining pellets were re-extracted with 1 mL of less-soluble proteins buffer (less-soluble PB: 0.1 M NaOH, 1% sodium dodecyl sulphate, 0.5% β-mercaptoethanol dissolved in distilled water), by vortexing tubes for 2 min and subsequently boiling them at 60 °C for 15 min. After centrifugation (10 min, 1500 × *g*), supernatants were harvested (I extract), while pellets were re-extracted in 0.5 mL of less-soluble PB as described above. Samples were then centrifuged (10 min, 1500 g) and the supernatants (II extract) were added to the I extract obtaining a fraction with less-soluble proteins (F2), which was rapidly frozen in liquid N_2, and kept at − 20 °C until analyses. The quantitative estimation of proteins, expressed in terms of percentage of algal dry weight (%DW) and of content per algal culture volume (g_{DW} L^{-1}), was determined with a modified Lowry's method, suitable for membrane protein determination (Markwell et al. 1981). Bovine serum albumin (BSA) was used as the standard (Sigma, USA).

Isolation of thylakoid membranes

Thylakoid membranes of microalgal samples were isolated according to Giovanardi and coworkers (2017), based on a slightly modified protocol reported by Järvi et al. (2011). For extraction, after 1 h of dark incubation, an aliquot of 300 mL of algal cultures in the stationary phase of growth (18 days of cultivation) was harvested by centrifugation at 600 × *g* for 10 min at 4 °C. Pellets were transferred into an ice-cold mortar containing sand quartz and cells were grinded in the presence of liquid N_2. Subsequently, the lysate was resuspended in a grinding P1 buffer (330 mM sorbitol, 50 mM Tricine-KOH pH 7.5, 2 mM Na_2EDTA pH 8.0, 1 mM $MgCl_2$, 5 mM ascorbate, 0.05% bovine serum albumin, 10 mM NaF) and moved into 15-mL tubes. Samples were centrifuged at 300 × *g* for 5 min at 4 °C and then at 700 × *g* for 5 min at the same temperature, in order to remove sand quartz and cell debris. Pellets were discarded, while the thylakoids contained in the supernatant were collected by centrifugation at 7000 × *g* for 10 min at 4 °C. After that, the supernatant was discarded, and thylakoids were resuspended in 1 mL of P2 shock buffer (5 mM sorbitol, 50 mM Tricine-KOH pH 7.5, 2 mM Na_2EDTA, 5 mM $MgCl_2$, 10 mM NaF) and centrifuged at 7000 × *g* for 10 min at 4 °C. Then, the supernatant was removed and around 100 µL of P3 storage buffer (100 mM sorbitol, 50 mM Tricine-KOH pH 7.5, 2 mM Na_2EDTA pH 8.0, 5 mM $MgCl_2$, 10 mM NaF) was added to the pellet. Thylakoid samples were rapidly frozen in liquid N_2 and stored at − 80 °C until further analyses. Manipulation of samples was always performed on ice and in very dim safe light. Quantification of chlorophylls (Chls) in thylakoid samples was performed according to Porra et al. (1989).

Denaturing gel electrophoresis

The two total protein fractions (i.e. F1 and F2) and the thylakoid membrane proteins were characterised by SDS-PAGE (15% acrylamide resolving gel containing 6 M urea), according to Laemmli (1970) with minor modifications. For SDS-PAGE gels, 10 or 15 µg of proteins was loaded in each lane respectively, whereas, for thylakoid membrane proteins, samples were loaded on equal Chls basis (2 µg in each lane). After electrophoresis, proteins were visualised by Coomassie staining (0.1% Coomassie Brilliant Blue R250, 7% acetic acid, 40% MeOH in distilled water) following routine protocols. ImageJ software (Version 1.52e, National Institutes of Health, Bethesda, USA) was used for quantitative densitometric analysis of gel bands. Main thylakoid protein component (PSI, CP43, CP47, D2, D1 and the Light-Harvesting Complex of PSII, LHCII) bands were identified on the basis of the molecular weight. The quantitative analysis of the electrophoretic gels was performed using ImageJ software (imagej.nih.gov), following the manufacturer's instructions. In particular, it was used to generate lane profile plots and to quantify the band intensities. To this purpose, a horizontal rectangular selection of each band of interest was done across four neighbouring lanes, and the background due to Coomassie staining was subtracted before measuring the band intensity.

Blue Native PAGE and second dimension electrophoresis

BN-PAGE was performed as described by Rokka and collaborators (2005), with minor modifications. Thylakoids containing 8 µg Chls were resuspended in medium A (25 mM Bis–Tris-HCl, pH 7.0 and 20% w/v glycerol and 0.25 mg mL^{-1} Pefabloc), thereafter an equal volume of 1.5% (w/v) dodecyl β-D-maltoside (Sigma), freshly prepared in medium A, was added. Thylakoids were then solubilised and centrifuged at 4 °C (18,000 × *g* for 15 min). The supernatant was supplemented with 1/10 volume of SB buffer (100 mM BisTris-HCl, pH 7.0, 0.5 M ε-amino-n-caproic acid, 30% w/v sucrose and 50 mg mL^{-1} Coomassie Brilliant Blue G250 dye). Samples were loaded on 5–12.5% gradient of acrylamide gel and first dimension (1D) electrophoresis was performed at 0 °C for 6 h by gradually increasing the voltage from 50 to 200 V, using an Owl Separation Systems (model P8DS, USA). Anode (50 mM BisTris/HCl pH 7.0) and cathod (50 mM Tricine, 15 mM BisTris/HCl pH 7.0, 0.01% Coomassie Brilliant Blue G250 dye) buffers were used according to Järvi et al. (2011). Quantification of band volume was performed with ImageJ software. After BN-PAGE, the lanes were cut out and incubated for 1 h in 10% SDS Laemmli buffer containing 5% (v/v) β-mercaptoethanol. Then, separation of the protein subunits of photosynthetic complexes was performed with SDS-PAGE (15% acrylamide resolving gel containing 6 M urea) in second dimension (2D). After electrophoresis, proteins were visualised by silver staining (Chevallet et al. 2006).

Data treatment

Data were processed with GraphPad Prism 9 (Graph Pad Software, USA). In each case, means ± standard deviations for *n* number of samples are given. The statistical significance of differences was determined by one-way ANOVA followed by a multiple comparison test (Tukey's test). A significance level of 95% ($p < 0.05$) was accepted.

Results

Evaluation of growth

The four green algae, *C. protothecoides*, *C. vulgaris*, *S. acutus* and *N. oleoabundans*, cultivated under identical culture

conditions, showed similar growth kinetics (Fig. 2a and its insert). Despite cultures started from different cell densities as the obvious consequence of algae inoculation, which was set up on an OD_{750} basis, all samples promptly entered the exponential phase and grew with very similar growth rates, ranging between 0.6 and 0.7 day^{-1} (time interval for all cultures, 0–5 days; Fig. 2a with its insert, and 2b). After this period, all cultures underwent a 5–7-day-long late exponential phase, and then entered the stationary phase of growth, reaching different, but not significant, final cell densities, with higher values for *N. oleoabundans* (about 14×10^6 cells mL^{-1}) as compared to the other cultures (about $7–9 \times 10^6$ cells mL^{-1}; ANOVA, $p > 0.05$) (Fig. 2a). These different final cell densities did not coincide with different OD_{750} values (Fig. 2a, insert; ANOVA, $p > 0.05$). Moreover, despite *C. protothecoides*, *C. vulgaris* and *S. acutus* reached lower cell densities than those observed for *N. oleoabundans*, they yielded higher biomass (61, 32 and 50% higher than that of *N. oleoabundans*, respectively) (Fig. 2c). The pH of culture media showed the following differences between samples: (1) *C. vulgaris*, *S. acutus* and *N. oleoabundans* gave pH curves almost perfectly overlapping the shape of growth curves, with *Neochloris* maintaining lower values of pH with respect to the other two algae; (2) at 10 days of cultivation, *C. protothecoides* showed one pH peak, which was followed by a reduction to stable values around 10 during the following days of cultivation (Fig. 2d). Overall, the highest pH values were recorded for *S. acutus* cultures at 14–18 days of cultivation.

Photosynthetic pigment content

On the whole, concentration of photosynthetic pigments inside cells of all samples increased with cultivation time, as expected for growing algae cultures due to self-shading, and reached different final concentrations (Fig. 3a–d). Interestingly, despite the general increasing trend, *S. acutus* showed an initial evident reduction in pigment concentration in the time interval 0–5 days of cultivation. Regardless of this initial and temporary decline, this Trebouxiophycea showed the highest Chl*a* concentration as compared to the other species (1.3, 1.7 up to 2.5 times higher values than in *C. protothecoides*, *C. vulgaris* and *N. oleoabundans*, respectively, at time 18 days) (Fig. 3a). Differently, the highest Chl*b* content was observed in both *S. acutus* and *C. protothecoides* (Fig. 3b). Overall, *S. acutus* showed the highest total Chls (Chl_{TOT}) content as compared to the other species (ca. 1.2, 1.6 and 2.3 times higher than in *C. protothecoides*, *C. vulgaris* and *N. oleoabundans*, respectively) (Fig. 3c). Similar to that observed for Chl*a* and Chl_{TOT} content, *S. acutus* also contained the highest Car concentrations as compared to the other strains

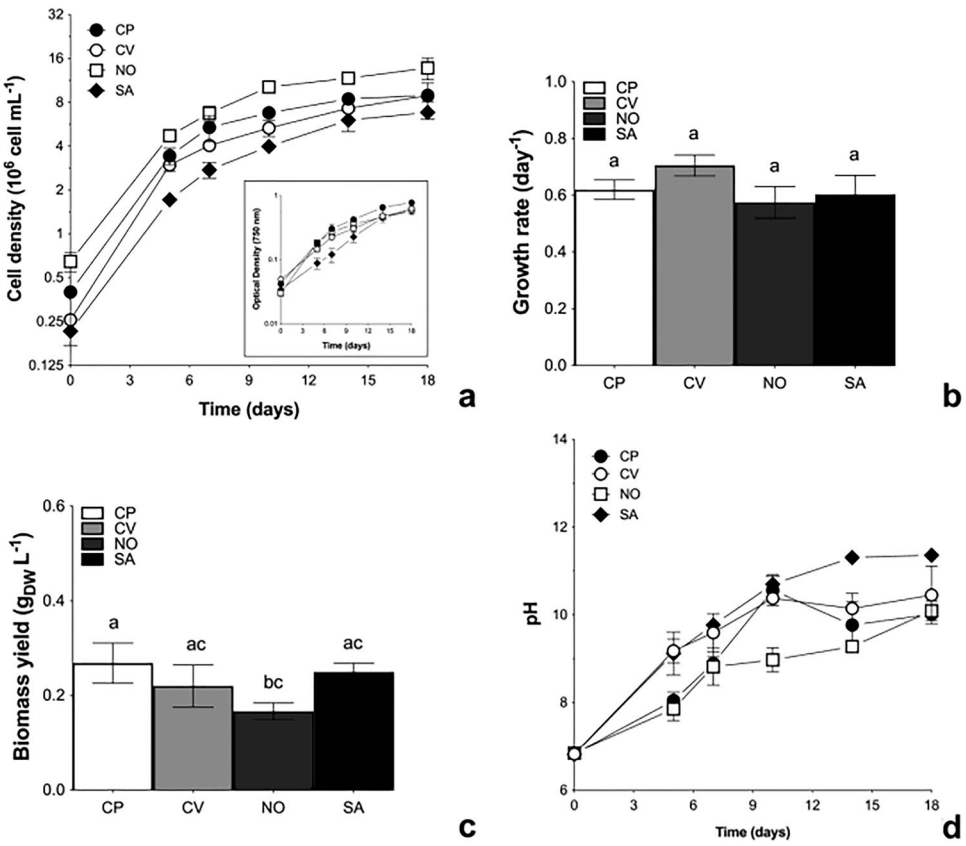

Fig. 2 Growth parameters of *C. protothecoides*, *C. vulgaris*, *N. oleoabundans* and *S. acutus*. **a** Growth curves and **b** growth rates ($\mu = day^{-1}$), calculated during the exponential phase (0–5 days). **c** Dry biomass yields at the 18th day of cultivation. **d** Trend of pH during cultivation. Line symbols in (**a**) and (**d**): *C. protothecoides* (CP), filled circles; *C. vulgaris* (CV), empty circles; *N. oleoabundans* (NO), empty squares; *S. acutus* (SA), filled diamonds. Histograms in (**b**) and (**c**): *C. protothecoides* (CP), white; *C. vulgaris* (CV), light grey; *N. oleoabundans* (NO), dark grey; *S. acutus* (SA), black. Values are represented as means ± s.d. ($n = 3$). ANOVA, $p < 0.05$. Different superscripts denote significant ($p < 0.05$) differences between samples

(ca. 1.3–1.4 times higher than in *C. protothecoides*, *C. vulgaris*, and ca. 2.4 times higher than in *N. oleoabundans*) (Fig. 3c, d). The general increase in pigment content resulted in relatively stable and species-specific photosynthetic pigment molar ratios (Fig. 3d, e). The Chl*a/b* ratio was generally higher in *S. acutus* (ca. 3) as compared to the other species (ca. 2.5) (Fig. 3e). In parallel, during the entire cultivation time, *S. acutus* showed almost a constant Chl_{TOT}/Car ratio (ca. 6), while in the other species, the same molar ratio was subjected to an evident increase until the 5th day. Subsequently (5–18 days), in *C. protothecoides* and in *N. oleoabundans*, Chl_{TOT}/Car ratio tended to settle at similar values (about 5.5–5.8), also similar to those of *S. acutus*, while in *C. vulgaris*, it gradually decreased down to about 4.5 (ANOVA, $p < 0.05$) (Fig. 3f).

At the end of the cultivation time, when also total and thylakoid proteins were analysed, the pigment content was also evaluated as percentage of algal dry biomass (%DW; Fig. 3g, h) to give a more exhaustive datum for biotechnological applications of the algal biomass. Chl_{TOT} contents ranged between 3.8%DW, as the lowest value, for *N. oleoabundans*, and 5.8%DW, the highest one, for *C. vulgaris* and *S. acutus*; *C. protothecoides* showed an intermediate value (4.9%DW) (Fig. 3g). Differently, the Car content showed very evident differences among samples (Fig. 3h). In detail, *C. vulgaris* reached the lowest Car content (0.10%DW) as compared to the other species (ca. 3.5, 4 and 7 times lower than values obtained from *C. protothecoides*, *N. oleoabundans* and *S. acutus*, respectively) (Fig. 3h).

Maximum quantum yield of PSII

The maximum quantum yield of PSII (F_V/F_M ratio) was monitored during the experiment to compare the photosynthetic efficiency of each species (Fig. 4). No significant differences were reported among samples at 5, 7 and 10 days of cultivation (Fig. 4). In detail, *C. protothecoides* tended to give higher values of F_V/F_M as compared to the other algae, but the values differed significantly only at time 0, 14 and 18 days (ANOVA, $p < 0.05$). In particular, at the 14th day of cultivation, while *C. protothecoides* was characterised by a F_V/F_M of about 0.78, *C. vulgaris* and *S. acutus* showed F_V/F_M values around 0.74–0.75, and *N. oleoabundans* gave the lowest one, ca. 0.71 (ANOVA, $p < 0.05$). At the end of the experiment, *C. protothecoides* still showed the highest values of the PSII maximum quantum yield (0.78) as compared to all other samples (0.71–0.72; ANOVA, $p < 0.05$). Despite the abovementioned differences, overall results showed that all selected species had F_V/F_M values that, during the cultivation time, varied in a short range of values from 0.65 to 0.75, not attributable to stressed cultures (Fig. 4).

Total protein content and pattern

In present research, due to the different morphology and cell characteristics of the four examined microalgae (not shown), preliminary tests using various protocols for protein extraction were performed to find the more suitable and employable one for all the four Chlorophyta (for details, see: Meijer and Wijffels 1998; Ivleva and Golden, 2007; Pruvost et al. 2011; Popovich et al. 2012; Serive et al. 2012; Baldisserotto et al. 2016). Based on the results obtained from different extraction methods (data not shown), the procedure proposed in the present work allowed obtaining a successful extraction of total proteins from all samples, independent of their morphological and biochemical characteristics.

In this study, a fraction containing easily extractable soluble proteins (F1) and a fraction with less-easily extractable ones (F2), including transmembrane proteins, were extracted from the four Chlorophyta species.

As shown in Table 1, the four green microalgae showed some differences in the final total protein content. In detail, *S. acutus* showed the highest value of total protein content (53.2%DW) as compared to the other species (47, 9 and 8% higher than in *C. protothecoides*, *C. vulgaris* and *N. oleoabundans*, respectively). *Scenedesmus acutus* was also characterised by the highest total protein content in the culture ($13.3\ g\ L^{-1}$) (Table 1).

Both fractions were also screened with SDS-PAGE analyses to obtain a qualitative comparison of protein extracts for the four Chlorophyta. Coomassie-stained gels revealed that the number and intensity of protein bands were different among the four species, independent of the fraction (i.e. with more or less easily extractable soluble proteins). Moreover, the F2 fraction gave the best results in terms of quality and resolution of protein bands as compared to the F1 fraction (Fig. 5). In all samples, the extracted proteins were resolved into distinct bands, mainly from 76 to 12.3 kDa. Based on literature data, the distinct band with a molecular mass of about 55–56 kDa was assignable to the ribulose-1,5-bisphosphate carboxylase/oxygenase (RuBisCO) large subunit (Spreitzer 1993; Park et al. 1999) and the protein bands below 30 kDa mainly corresponded to subunits of the LHCII (Bennett 1991) (Fig. 5). Interestingly, the pattern of the easily extractable soluble protein fraction (F1), which represented only a very minor component in all algae cultures (Table 1) and appeared poorly defined, showed differences in bands among all algae (Fig. 5a). However, the main results derived from the SDS-PAGE analysis of F2 fraction, with the less easily extractable soluble proteins (Fig. 5b). In this sample, the protein pattern was overall similar within the same algal class. The two Chlorophyceae (*C. protothecoides* and *C. vulgaris*) showed similar protein profile each other; the same observation was applicable to the two Trebouxiophyceae (*N. oleoabundans* and *S. acutus*) as well. Indeed,

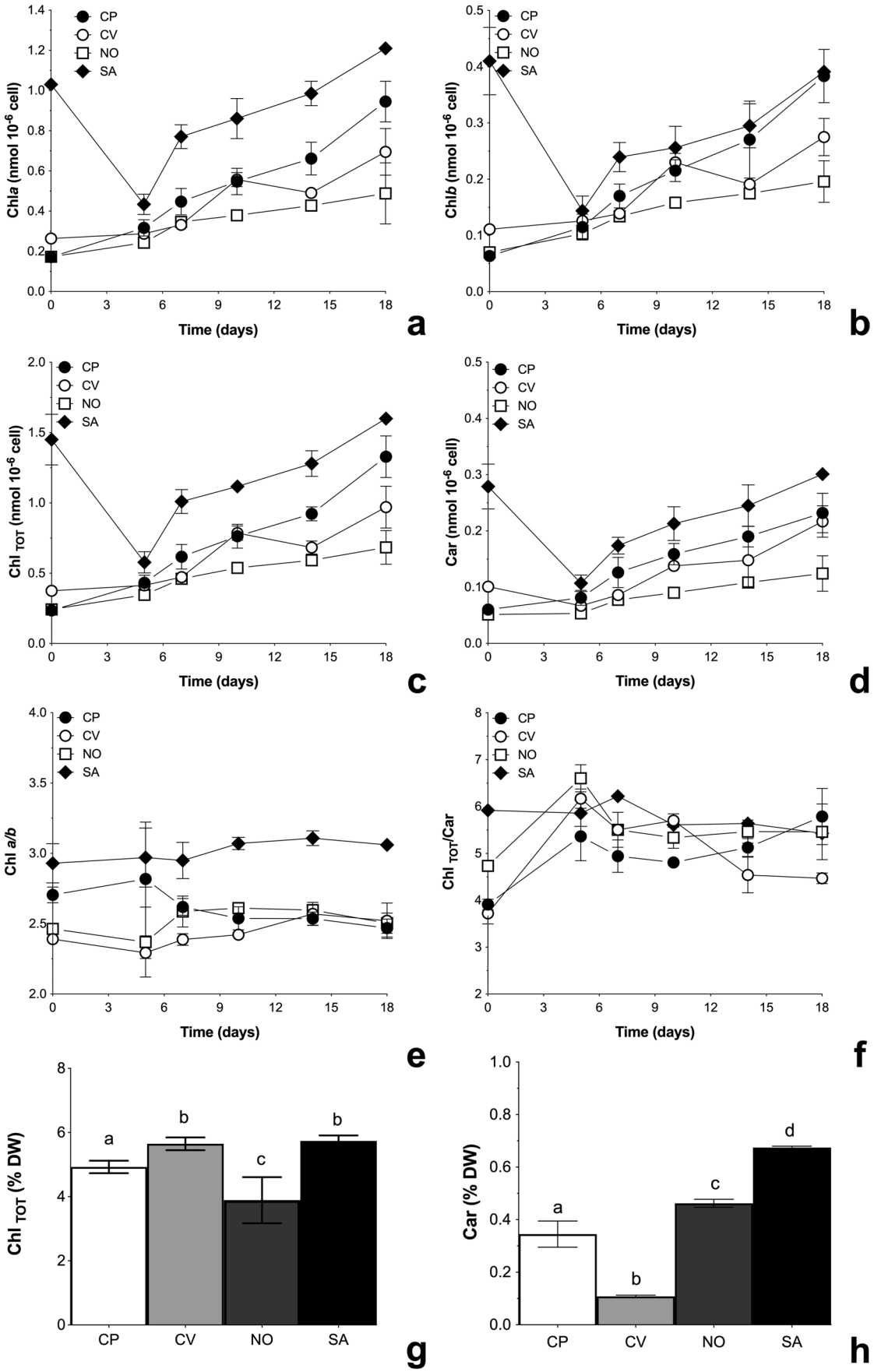
CP
CV
NO
SA
Chla (nmol 10-6 cell)
Time (days)
a
Chlb (nmol 10-6 cell)
b
Chl TOT (nmol 10-6 cell)
c
Car (nmol 10-6 cell)
d
Chl a/b
e
Chl TOT/Car
f
Chl TOT (% DW)
g
Car (% DW)
h

◂**Fig. 3** Photosynthetic pigment content and their molar ratios in *C. protothecoides, C. vulgaris*, *N. oleoabundans* and *S. acutus*. **a**–**f** Time-course variations of Chl*a* (**a**), Chl*b* (**b**), total Chls (Chl_{TOT}; **c**) and Car (**d**) concentrations, expressed as $nmol_{PIG}$ 10^{-6} cells, and the parallel Chl *a*/*b* (**e**) and Chl_{TOT}/Car (**f**) molar ratios. (**g**, **h**) Chl_{TOT} (**g**) and Car (**h**) content, expressed as percentage of dry weight biomass (%DW), at the 18th day of cultivation. Line symbols in (**a**–**f**): *C. protothecoides* (CP), filled circles; *C. vulgaris* (CV), empty circles; *N. oleoabundans* (NO), empty squares; *S. acutus* (SA), filled diamonds. Histograms in (**g**) and (**h**): *C. protothecoides* (CP), white; *C. vulgaris* (CV), grey; *N. oleoabundans* (NO), dark grey; *S. acutus* (SA), black. Values are means ± s.d. ($n = 3$). ANOVA, $p < 0.05$. Different superscripts denote significant ($p < 0.05$) differences between the samples

in algae from both classes, resolution of LHCII was peculiar (Fig. 5b). In *C. protothecoides* and *C. vulgaris*, the LHCII was mostly represented by one evident band, while it was resolved into two bands with similar intensity in the other two algae.

Thylakoid protein complexes

The SDS-PAGE and 2D BN/SDS-PAGE analyses were performed to obtain information on thylakoid protein complexes and their native organization inside the photosynthetic membrane in the four Chlorophyta (Figs. 6 and 8). The assignment of major bands belonging to abundant thylakoid proteins conserved over the entire green lineage was based on approximate molecular mass (Minagawa and Takahashi 2004; Dekker and Boekema 2005); furthermore, it is consistent with relatively recent thylakoid protein profiles and immunodetections in *N. oleoabundans* (Giovanardi et al. 2017). On the basis of SDS-PAGE analysis, the densitometric profile was obtained for each species (Fig. 6a, b). In each lane, the first conspicuous band corresponded to the major photosystem I (PSI) polypeptides PsaA/PsaB (around 62 kDa) (Fig. 6a, b). As regards PSII, the band around 43 kDa was assignable to its light-harvesting protein CP43, and the two homologous proteins of nearly 30 kDa corresponded to D1 and D2 subunits of the reaction centre of PSII core. Finally, the LHCII was resolved in four or five separated bands below 30 kDa. In general, the two Trebouxiophyceae, *C. vulgaris* and *C. protothecoides*, shared a very similar thylakoid membrane protein pattern as compared to the other two species, which instead showed differences mainly in the bands corresponding to the LHCII proteins (Fig. 6). For semi-quantitative comparison between the four green algae, the relative amount (band volume ratio) of different photosynthetic proteins in the thylakoid complexes was quantified. The band volumes were used to calculate band volume ratios (Fig. 7). The LHCII/D2 ratio, which reflects the abundance of LHCII as compared to PSII cores, was comparable within the same classes of Chlorophyta: it was lower in the two Trebouxiophyceae than in the two Chlorophyceae, with values around 6 and 8, respectively (Fig. 7a). The PSI/D2 ratio, which provides information about stoichiometric variations involving the two photosystems, was markedly lower in *S. acutus* as compared to all other species (−40 to −45%; ANOVA, $p < 0.05$) (Fig. 7b). Finally, the LHCII/PSI band volume ratio, which reflects the potential LHCII availability also for PSI, was subjected to species-specific variability (Fig. 7c). The two Chlorophyceae, *N. oleoabundans* and *S. acutus*, showed values of about 4 and 2.2, respectively, while the two Trebouxiophyceae, *C. vulgaris* and *C. protothecoides*, recorded values below 2. Due to the abovementioned differences in availability of LHCII for the photosystems, it was evaluated if the stoichiometry of photosynthetic proteins had an impact on native interactions; thus, thylakoid membranes were mildly solubilised using dodecyl β-D-maltoside and separated by BN-PAGE.

All the four green microalgae exhibited the presence of four distinct bands, ordered from I to IV, and a heavier and less defined band, called megacomplex (MC), on the uppermost part of the gel (Fig. 6c). The latter MC band was particularly evident in *S. acutus* (Fig. 6c). BN-PAGE profile appeared different between the two Chlorophyceae, while it was very similar for the two Trebouxiophyceae (Fig. 6c). Identification of complexes of the Chlorophyceae *N. oleoabundans* was done based on a published BN-PAGE profile from the same alga and supported by 2D BN/SDS-PAGE pattern (Giovanardi et al. 2017) (Fig. 8a). In detail, the lowest band (I) was attributed to LHCII monomers, band II to LHCII trimers, band III to PSII monomers and band IV to supercomplexes of PSI and LHCs (Fig. 6c). In *N. oleoabundans*, the LHCII was mainly found in monomeric form (Figs. 6c and 8a). In the 2D gel, the PSII was revealed by its subunits CP47, CP43, D2 and D1 (Fig. 8a). PSII was found almost completely as a monomer in band III (Fig. 8a). However, as already observed by Giovanardi et al (2017), a very faint amount of PSII was present as a dimer co-migrating with PSI (band III^{I} in Fig. 8a), slightly lighter than the PSI-LHCI complex. Some faint PSII components also co-migrated with PSI in band IV: these are most probably ascribed to PSII dimers associated with one LHCII trimer (as shown in Giovanardi et al. 2017, band IV has approximately the same weight of C_2S complex of *Arabidopsis*). The high molecular weight region including MC actually was comprised of a series of complexes formed by PSI and/or PSII with their antennae. The lightest components of the series were probably assignable to co-migrating individual supercomplexes of PSI or PSII. Conversely, the heaviest components could include both photosystems in native megacomplexes. A clear spot aligned with PSI-LHCI at about 130 kDa was also resolved from bands IV and, to a lesser extent, MC (Fig. 8a). Because of its weight and alignment with PSI, it corresponded to PsaA/PsaB heterodimer, as also observed

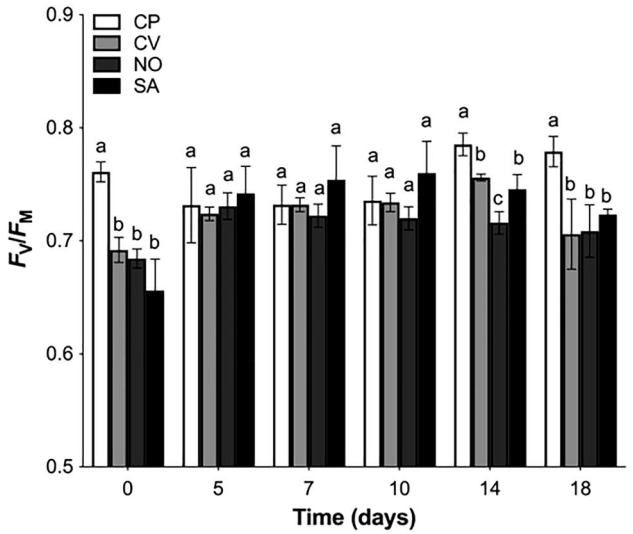

Fig. 4 Time-course variations of PSII maximum quantum yield (F_V/F_M ratio) in *C. protothecoides* (CP; white), *C. vulgaris* (CV; light grey), *N. oleoabundans* (NO; dark grey) and *S. acutus* (SA; black). Values are represented as means ± s.d. ($n=3$). ANOVA, $p<0.05$. Different superscripts denote significant ($p<0.05$) differences between the samples within each day of cultivation

in *Chlamydomonas* sp. UWO (Nelson and Ben-Shem 2004; Szyszka-Mroz et al. 2015). Finally, on the right side of the 2D BN/SDS-PAGE, large quantities of free proteins with different molecular weights were evident (Fig. 8a).

Overall, the 2D BN/SDS-PAGE profiles highlighted some evident differences comparing the samples (Fig. 8). In the other Chlorophycea, *S. acutus*, the presence of PSII subunits was more included in the MC band, which was much more represented than in the other algae (Figs. 6c and 8b). In particular, the heaviest complex was very well resolved with its components of PSI, PSII and LHCs. The PSI-LHCI band in the 2D gel was mainly formed by PsaA/PsaB heterodimer (Fig. 8b). LHCII was almost equally distributed between the monomeric and the trimeric forms (Fig. 8b). Solubilised stripes from *S. acutus* thylakoids produced a large amount of free single proteins at the right side of the SDS-PAGE gel in second dimension likewise in *N. oleoabundans* (Fig. 8b).

The two Trebouxiophyceae shared a very similar BN-PAGE profile (Fig. 6c); as a reference sample, *C. vulgaris* stripe was solubilised and run in 2D for native band analysis (Fig. 8c). As compared to *N. oleoabundans* samples, in *C. vulgaris*, LHCII was more represented in the trimeric form than in the monomeric one, PSII was similarly represented mostly by monomers, while co-migrating PSI with PSII dimers (from a III^I band) and MC were not abundant (Fig. 8c). PsaA/PsaB heterodimer of 130 kDa and free proteins on the right side of the gel also characterised the 2D profile in this alga (Fig. 8c).

Discussion

Modern molecular studies have revealed that the green algal classes Chlorophyceae and Trebouxiophyceae, which are characterised by similar morphological shape but also by a remarkable diversity of physiological and biochemical constraints, evolved in independent phylogenetic lineages as the result of convergent evolution within the Chlorophyta Phylum (Leliaert et al. 2012; Krienitz et al. 2015). As highlighted by the present research study, the specific variability (and similarities) of each strain clearly emerges comparing not only growth but also the biochemical profile and characteristics of the examined algae.

The monitoring of microalgal growth and the knowledge of biological characteristics of these micro-organisms are fundamental issues to improve the performance of cultures in biotechnological fields (Havlik et al. 2013; Maglie et al. 2021). Growth, photosynthetic pigment and protein content represent species-specific aspects of microalgae but are influenced by culture conditions. Thus, our comparative study on four Chlorophyta species cultivated in the same culture conditions was helpful to better highlight biological differences among those species. However, it should be underlined that the present study was set up employing laboratory culture conditions; for an industrial mass cultivation

Table 1 Protein content, expressed as percentage of dry weight biomass (%DW) and gram per litre (g L^{-1}), at the 18th day of cultivation in *C. protothecoides*, *C. vulgaris*, *N. oleoabundans* and *S. acutus* samples. Values are represented as means ± s.d. ($n=3$). ANOVA, $p<0.05$

Strains	Easily extractable soluble proteins, F1		Less-easily extractable soluble proteins, F2		Total proteins	
	(%DW)	(g L^{-1})	(%DW)	(g L^{-1})	(%DW)	(g L^{-1})
Chlorella protothecoides	$3.4^{a}\pm0.4$	$0.91^{a}\pm0.13$	$32.7^{a}\pm4.9$	$8.7^{a}\pm0.3$	$36.1^{a}\pm5.2$	$9.6^{b}\pm0.5$
Chlorella vulgaris	$1.8^{b}\pm0.5$	$0.41^{b}\pm0.08$	$46.8^{ab}\pm5.9$	$10.5^{acd}\pm1.9$	$48.6^{ab}\pm6.5$	$10.9^{ab}\pm3.7$
Neochloris oleoabundans	$3.8^{a}\pm0.6$	$0.63^{ab}\pm0.13$	$45.7^{ab}\pm7.8$	$7.6^{bd}\pm0.55$	$49.5^{ab}\pm8.1$	$8.2^{b}\pm0.6$
Scenedesmus acutus	$1.1^{b}\pm0.1$	$0.26^{c}\pm0.04$	$52.1^{b}\pm4.2$	$13.0^{c}\pm0.9$	$53.2^{b}\pm4.3$	$13.3^{a}\pm0.1$

Different superscripts denote significant ($p<0.05$) differences between the means in columns of each protein fraction

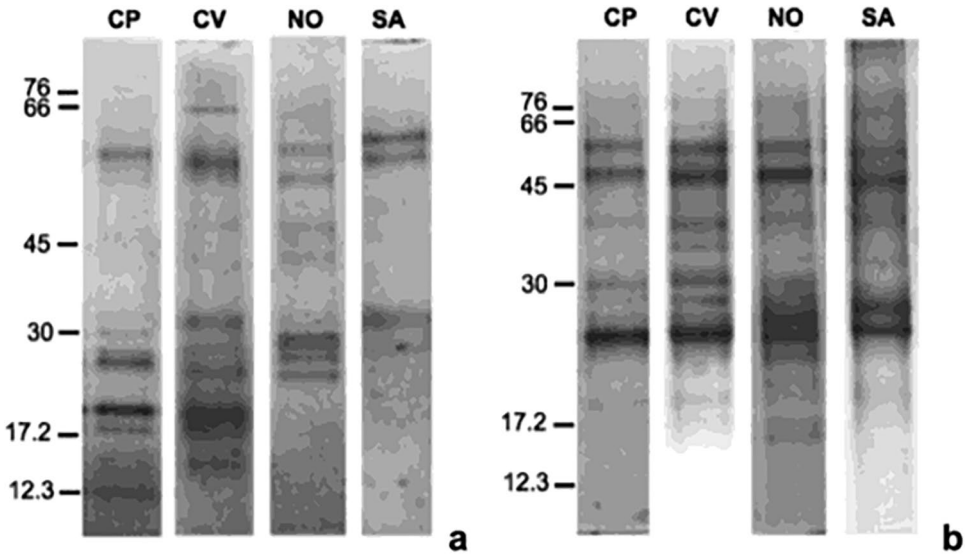

Fig. 5 **a** Coomassie-stained SDS-PAGE of the easily extractable, F1, and (**b**) less easily extractable, F2, soluble protein fractions of *C. prototheco-ides* (CP), *C. vulgaris* (CV), *N. oleoabundans* (NO) and *S. acutus* (SA). On each lane, 10 µg (**a**) and 15 µg of proteins (**b**) were loaded. Molecular weight (kDa) marker is reported on the left side of each figure

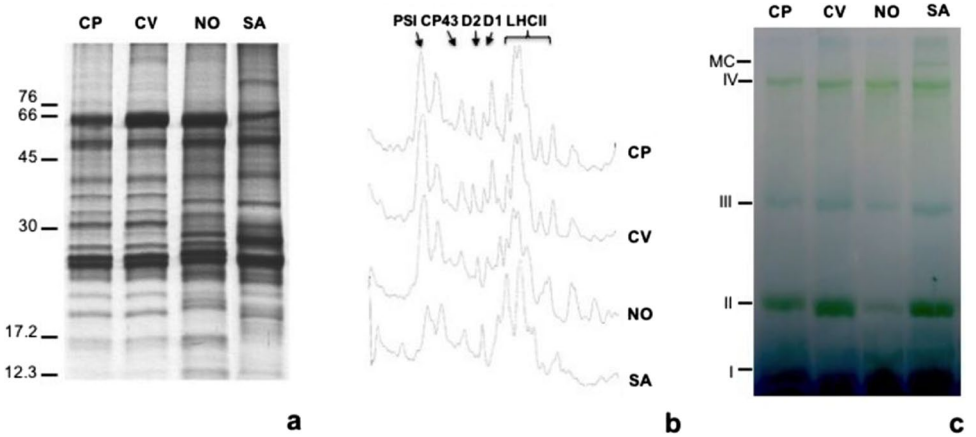

Fig. 6 **a** Coomassie-stained SDS-PAGE of thylakoid membrane proteins, **b** densitometric profiles and **c** distribution of different protein complexes in BN-PAGE profile of thylakoid membranes of *C. protothecoides* (CP), *C. vulgaris* (CV), *N. oleoabundans* (NO) and *S. acutus* (SA). In **a**, on each lane, 2 µg of Chl was loaded. Molecular weight (kDa) marker is reported on the left side of the gel. In **c**, purified thylakoids were solubilised with 1.5% (v/v) dodecyl β-D-maltoside, loaded on an equal chlorophyll (8 µg) basis and separated on 5–12.5% gradient native gel. The position of major complexes is indicated by labels on the left side of the gel

of these algae, specific scale up tests are needed to adjust cultivation settings and systems. In this perspective, our work gives useful basic biological information of the tested algae in view of future massive productions.

In biotechnological applications of microalgae, growth is usually quantified by measuring the optical density (OD at different wavelength: usually 750 or 680 nm) or the biomass concentration as DW per litre of algal culture; direct cell counts at the microscope are less common (Moheimani 2013). In addition, the monitoring of pH values of culture media is an indirect way to monitor algal growth. In this regard, the pH of culture media is attributed to the species-specific assimilation and release of CO_2 during photosynthesis and respiration, respectively, and is correlated to the growth of algae (Khalil et al. 2010; Moheimani 2013). OD is frequently used as a rapid and non-destructive indirect measurement of biomass or cell density, but its use to indirectly estimate cell density or biomass can bring artefacts, since the OD of living cells varies during growth phases and among treatments. DW determination is a convenient, but time- and material-consuming method for growth evaluations. Conversely, the direct count of cells is time consuming and needs expertise by the operator. OD and DW methods generate mistakes in the growth estimation being closely dependent on culture conditions, different growth phases and morphological state of the cells, namely cell size and shape (Griffiths et al. 2011; Baldisserotto et al. 2016). So, for biological studies, it is appropriate to integrate OD and

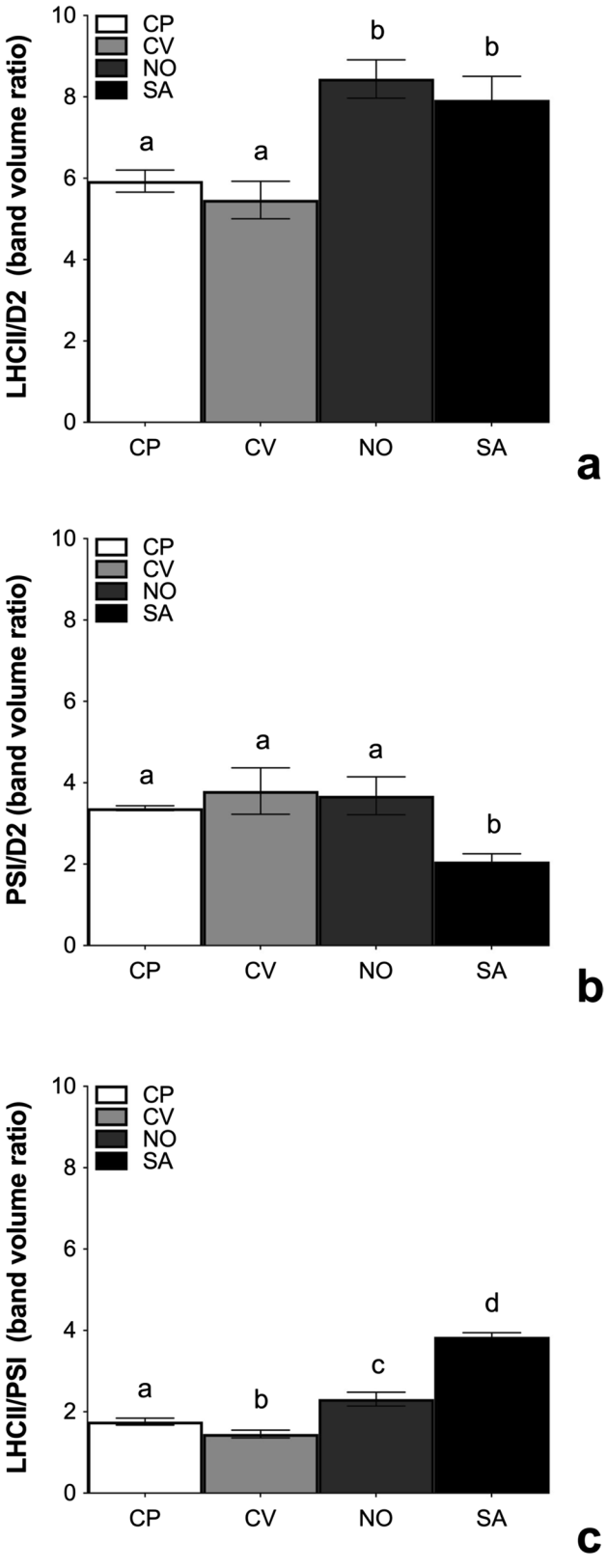

Fig. 7 Semi-quantitative analyses of (**a**) LHCII/D2, (**b**) PSI/D2 and (**c**) LHCII/PSI band intensities (band volume ratio) in thylakoid membranes of *C. protothecoides* (CP; white), *C. vulgaris* (CV; light grey), *N. oleoabundans* (NO; dark grey) and *S. acutus* (SA; black). Values are represented as means ± s.d. ($n = 3$). ANOVA, $p < 0.05$. Different superscripts denote significant ($p < 0.05$) differences between the samples

DW with cell counts. This is clearly confirmed in this study, where all parameters have been analysed for growth estimation of algae. The four selected green algae showed similar growth kinetics and rates. Values of the latter parameter are close to the results reported for some other Chlorophyta species cultivated at irradiance similar to those used in this study (Singh and Singh 2015). However, by comparing OD, cell density and DW at the end of the experiment, it emerges that these parameters are not directly correlated with each other, being, for example, the same OD produced by different cell densities and biomass. This discrepancy descends from different morphological characteristics of the microalgae (example, cell size and shape) (Leliaert et al. 2012), but can have important implications when studying microalgae, especially in view of the potential application of their biomass, and when comparing literature data on growth. Moreover, in all cases, the pH value of culture media during cultivation displayed a diverse pattern among samples. According to previous studies (Moheimani 2013; Difusa et al. 2015; Sabia et al. 2015), under unregulated pH conditions, microalgae showed an overall increase in the pH of the medium with time, which is attributed to the consumption of CO_2 during the photosynthetic process and to protons uptake (Villarejo et al. 1995; Zerveas et al. 2021). For a better study of algal growth, the PSII maximum quantum yield was also measured. The photochemical activity of PSII is widely used to estimate the physiological state of microalgae, being very sensitive to stressful conditions (White et al. 2011; Schuurmans et al. 2015), and, therefore, is also employed to follow and optimise microalgae growth performance (Schuurmans et al. 2015). The results stated that the selected four Chlorophyta maintained a nearly invariable and optimal PSII photochemistry throughout the experiment, thus excluding the occurrence of major stresses (White et al. 2011). So, cultures were further analysed in relation to their biotechnological impact and biological characteristics.

For the exploitation of microalgae especially in the food/feed sectors, besides growth, it is important to quantify the added value of biomass. Under autotrophic conditions, the more abundant molecules accumulated inside algae are photosynthetic pigments and proteins. Chlorophylls and carotenoids characterise all photosynthetic organisms, while RuBisCO is the major enzymatic protein in photosynthetic plant cells (including microalgal cells) and LHCII is the most abundant membrane protein on Earth (Crepin and Caffarri 2018). Both these classes of molecules have a double importance in a biotechnological perspective, since they represent a high percentage of the whole biomass

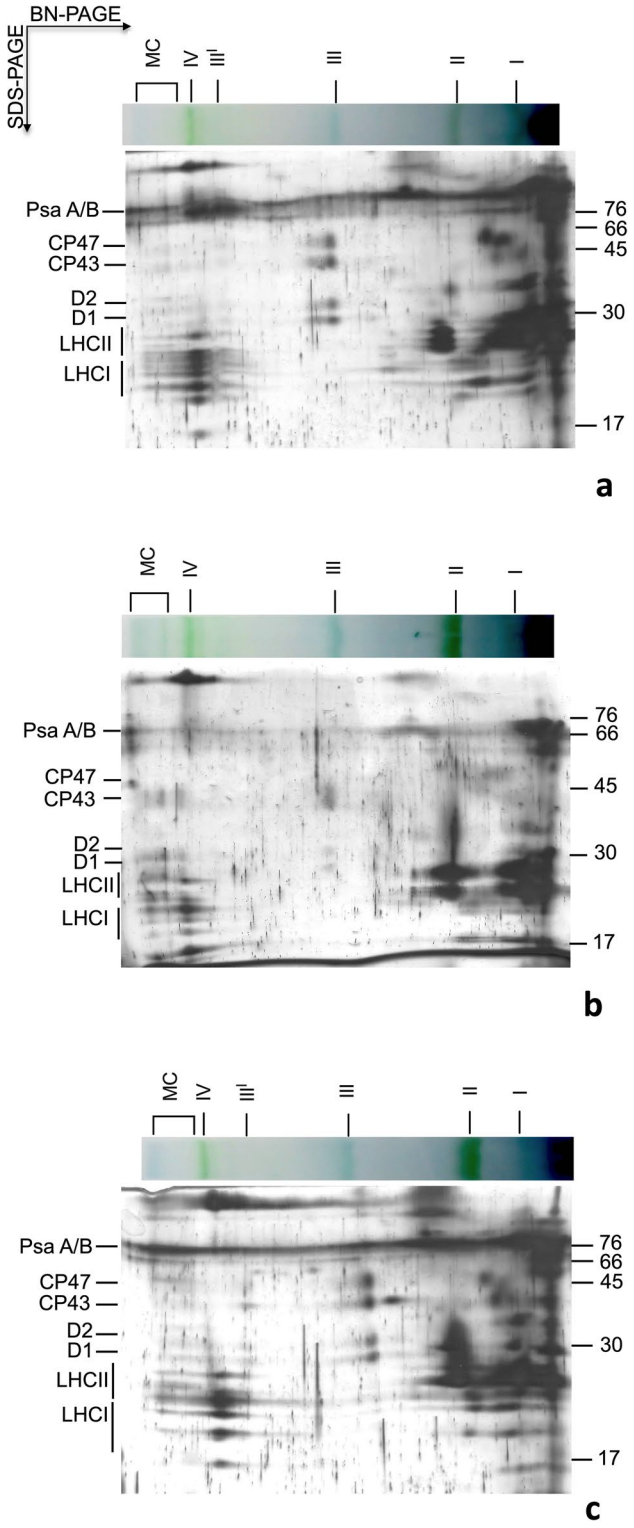

Fig. 8 2D BN/SDS-PAGE of protein complexes in thylakoid membranes of *N. oleoabundans* (**a**), *S. acutus* (**b**) and *C. vulgaris* (**c**). The BN-PAGE strips were treated with 10% (v/v) SDS and 5% (v/v) β-mercaptoethanol and denatured subunits were separated using SDS-PAGE. Second dimension gels were silver stained. Marker molecular weight (kDa) is indicated on the right side of the gels

(contributing to improve the nutritional and antioxidant properties of food, feed and supplements) and participate in photosynthesis (Crepin and Caffarri 2018; Di Stefano et al. 2018; Amorim et al. 2021). The pigment composition of photosynthetic microorganisms is linked to the phylogenetic position of the organism and to environmental constraints (Deblois et al. 2013). Differences in photosynthetic pigments among the tested Chlorophyta were mainly attributed to phylogenetic position since algae were cultivated under the same culture conditions. In detail, the specific variability of each strain clearly emerged comparing the time-course analysis of the photosynthetic pigment content on a cell basis, suggesting that each species developed a kind of a unique metabolic framework, certainly determined by their phylogenetic characteristics, together with their specific morpho-physiological state (Deblois et al. 2013). Additionally, differences in pigment content could also relate to the adaptive evolution to the original sampling locations, as especially inferred by the conspicuous differences observed between *S. acutus* and *N. oleoabundans*, which belong to the same phylogenetic branch. Indeed, *N. oleoabundans* was originally isolated from sand samples of the Saudi Arabian desert, while *S. acutus* from wastewater samples harvested in Northern Italy (Chantanachat and Bold 1962; https://ccala.butbn.cas.cz/en). Interestingly, from the biotechnological point of view, *S. acutus* produced the biomass with the highest content in Car, which can be oriented to various industrial applications. It is important to consider new sources of natural Car, because the global market of these pigments was projected to reach about 1.53 billion US$ in 2021 and considering that the use of synthetic Car has started to decline due to potential toxic effects of synthetic molecules (Ambati et al. 2019).

Parallel to photosynthetic pigments, the protein content and profile of the four Chlorophyta species were evaluated to highlight differences among samples. It is well known that a comparison of protein content in different microalgae is very difficult owing to the morphological and biochemical characteristics of each microalgae species but also to the several methods employed for protein extraction and quantification (Meijer and Wijffels 1998; Barbarino and Lourenço 2005; Safi et al. 2013; Ursu et al. 2014). As a preliminary step, several protein extraction methods were tested. The protein extraction procedure originally proposed by Ivleva and Golden (2007) was modified and allowed a better comparison of protein content. According to Buono et al (2014), disruption of the cell by vortexing with glass beads in the presence of SDS was an essential and effective extraction step to lyse the cell walls. The values of protein content here reported are consistent with literature data for green microalgae (Barka and Blecker 2016). Interestingly, *S. acutus* not only showed the highest value of protein content (53.2%DW) but also the highest total protein accumulation in the final culture (13.3 g L^{-1}) as compared to the other samples.

The SDS-PAGE analysis of total proteins showed a different pattern among algae, both considering the more and the less easily extractable fractions, F1 and F2. The main differences concerned LHCII subunits. Thus, the thylakoid membrane protein profile was studied more in detail by BN-PAGE and SDS-PAGE in first and second dimensions. The two Trebouxiophyceae shared a very similar thylakoid membrane protein pattern as compared to the other two species, which instead showed differences mainly in the bands corresponding to the LHCII proteins. To evaluate if the selected species showed significant variations in fundamental thylakoid complexes stoichiometry, the relative amount (band volume ratio) of some key proteins in the thylakoids were compared. Photosynthetic organisms regulate the stoichiometry of their photosynthetic complexes in response to variations of light intensity and spectral quality. To avoid light excess and to profitably make use of limiting light, plants and green algae have evolved different acclimation mechanisms that include both short-term and long-term responses (Anderson et al. 1995). Long-term acclimation responses generally involve changes in the stoichiometry of PSI versus PSII and the modulation of the LHCII (Humby and Durnford 2006; Wobbe et al. 2016). Among green algae, studies on acclimation mechanisms to light intensity are mainly on *C. reinhardtii*, which is widely explored as a photosynthetic model organism (Durnford et al. 2003; Mettler et al. 2014). However, contrasting results on acclimation behaviour have been reported in other green algae (Falkowski 1980; Finazzi and Minagawa, 2014) suggesting that acclimation mechanisms in green microalgae can be species-specific.

The PSI/D2 ratio showed that *S. acutus* had a markedly lower value as compared to all other species. The photosystems stoichiometry is modulated to balance the excitation between PSI and PSII; in a denser culture, such as that of *S. acutus*, the reciprocal shading of cells is expected to increase, leading not only to less available light intensity, but also to a relative enrichment in far-red. Since far-red is mainly absorbed by PSI, cells are expected to downregulate PSI in favour of PSII, as observed in *S. acutus*. More in general, the PSI/D2 ratio was negatively related to the biomass yields, indicating that this ratio reflected the acclimation to the available light quality, which in turn depends on the culture density (Büchel 2015; Wobbe et al. 2016). In the short-term, the excitation regulation of the two photosystems requires modulable associations of LHCII with PSI and PSII. The relative abundance of LHCII as compared to PSII cores was similar within the same class of Chlorophyta, but lower in the two Trebouxiophyceae than in the two Chlorophyceae. The LHCII/PSI ratio, which may reflect the availability of LHCII also for PSI (Falkowski 1980), had a species-specific variability, but with higher values for the two Chlorophyceae than for the two Trebouxiophyceae. In general, the two Chlorophyceae revealed a higher availability of LHCII antennae for both photosystems. In this paper, the functional distribution of LHCII between PSII and PSI was not determined. However, the BN/SDS-PAGE results are strongly suggestive of extensive and stable interactions with not only PSII, but also PSI, and, very probably, both photosystems at the same time. The heaviest MC, which is larger than known PSII-LHCII supercomplexes or PSI-LHCII state transition complexes, could be interpreted as an accidental aggregate (Galka et al. 2012). However, this is in contrast with ever-accumulating evidence about the existence of PSI-PSII-LHCII megacomplexes, which may mediate the interconnectivity between PSI and PSII, and play physiological roles in energy transfer between the two PSs, not necessarily linked to state transitions (Järvi et al. 2011; Grieco et al. 2015; Yokono et al. 2015, 2019; Ferroni et al. 2016; Giovanardi et al. 2017, 2018; Furukawa et al. 2019).

Applications of BN/SDS-PAGE technique in green microalgae have been mainly limited to *C. reinhardtii* and only seldom used for other microalgae, sometimes with uncertain results (Tran et al. 2009; Kantzilakis et al. 2007; Szyszka-Mroz et al. 2015; Giovanardi et al. 2017; Zhao et al. 2017; Garcìa-Cerdàn et al. 2019; van den Berg et al. 2020). However, by comparison with many published profiles of thylakoid complexes in higher plants (Kügler et al. 1997; Ferroni et al. 2014; Albanese et al. 2016), those of the tested microalgae were singularly poor of large complexes. This may depend on the harsh extraction protocol, required because of the robust cell walls of microalgae. Nevertheless, based especially on *C. reinhardtii*, the complexity of native thylakoid components in green algae can be as high as in land plants (Zhao et al. 2017; Umetani et al. 2018; Garcìa-Cerdàn et al. 2019; Kubota-Kawai et al. 2019; Nama et al. 2019; Calvaruso et al. 2020; van den Berg et al. 2020), different to that assumed or reported in previous years (Dekker and Boekema 2005; Kouřil et al. 2012). Therefore, the abundant free proteins on the right side of the gel are the unavoidable result of a harsh thylakoid isolation method. Although native interactions were not completely preserved, we highlighted some differences in the organization of the resolved thylakoid complexes of the four investigated green algae. By comparing the 2D BN/SDS-PAGE, each species showed some peculiarities in their thylakoid protein pattern. One evident difference was the prevalence of monomeric LHCII over the trimeric form in *N. oleoabundans*. Although it was reported that a population of monomeric LHCII exists in the photosynthetic membrane, where it acts as a dissipator of excess energy under high light conditions (Bielczynski et al. 2016), it is more realistic that very abundant monomeric forms of LHCII in green algae are caused by the isolation protocol and derive from the dissociation of trimers. Therefore, the relative abundance of monomers and trimers would reflect the recalcitrancy of microalgae to thylakoid isolation. A similar reason can explain the prevailing

monomeric PSII form, instead of the dimers. It is plausible that the characteristics of the cell wall could have influenced the extraction procedure. Indeed, in *N. oleoabundans*, the cell wall is formed by two layers (a thin outer layer and a thick inner one) (Rashidi and Trinidade 2018; Spain et al. 2021), while for *Scenedesmus* and *Chlorella* species, the cell wall can be composed by a third one (Voigt et al. 2014; Dixon and Wilken 2018; Spain et al. 2021). Furthermore, the cell wall composition is very different in these algae (Abo-Shady et al. 1993; Rashidi and Trinidade 2018). However, the attribution of different thylakoid complexes patterns only to methodological issues is too simplistic. In particular, it does not explain the resolution of high molecular weight complexes, which should be the most labile and in Angiosperms are not even preserved when dodecyl-maltoside is used as detergent (Järvi et al. 2011).

Only minor amounts of PSII dimers were observed/preserved in *C. vulgaris*, *S. acutus* and *N. oleoabundans*, and were well visibly organised in MC only in *S. acutus*, where the lighter complexes of the MC band were very likely due to co-migration of PSII-LHCII supercomplexes and PSI-LHCI. Differently, the heaviest complexes visible on the left side of the 2D BN/SDS-PAGE gel in *S. acutus* corresponded to various assemblages of PSI, LHCI and PSII-LHCII, and therefore were attributed to the PSI-(PSII)-LHCII megacomplexes. The comparison with MC bands of *Arabidopsis* reported in Giovanardi et al. (2017) supports this interpretation, since MC bands of algae samples were heavier than that of $C_2S_2M_2$ supercomplexes found in *Arabidopsis*. These results agreed with SDS-PAGE analysis and further showed that the higher LHCII/PSI ratio found in *S. acutus* can be linked to a quite complex interaction of LHCII with PSI, as discussed above. In particular, the pattern of protein complexes was richer in *S. acutus* as compared to the other species, which however showed the presence of PSI-(PSII)-LHCII megacomplexes. Finally, each species was characterised by a high molecular mass protein (> 130 kDa), which was assigned to components of a PSI-associated pigment-protein complex (Szyszka-Mroz et al. 2015).

Collectively, the results provide useful basic information for the exploitation of *C. vulgaris*, *C. protothecoides*, *N. oleoadundans* and *S. acutus* in biotechnological applications, such as the food/feed sector due to their richness in proteins. Even if only four species were studied, results have also highlighted the metabolic uniqueness of each strain, resulting in a non-self-explanatory comparison with the others, even the most related ones. It can be concluded that *S. acutus* is the most promising species to be used for biotechnological applications, due to its capability to produce satisfactory quantities of biomass, rich in proteins and photosynthetic pigments (mainly Car). Overall, it is shown that, in *S. acutus*, the major stability of the photosynthetic membranes very probably supports the productivity of a high-value biomass, confirming the importance of the organization of photosynthetic membranes to sustain the efficient growth of microalgae also in a biotechnological context.

Author contribution Conception or design of the work: Simonetta Pancaldi, Alessandra Sabia, Costanza Baldisserotto; data collection: Alessandra Sabia, Costanza Baldisserotto, Lorenzo Ferroni, Martina Giovanardi; data analysis and interpretation: Alessandra Sabia, Costanza Baldisserotto, Lorenzo Ferroni, Martina Giovanardi, Michele Maglie; technical support: Michele Maglie; drafting the article: Costanza Baldisserotto, Alessandra Sabia; critical revision of the article: Simonetta Pancaldi, Lorenzo Ferroni; final approval of the version to be published: Simonetta Pancaldi, Alessandra Sabia, Costanza Baldisserotto, Martina Giovanardi, Lorenzo Ferroni, Michele Maglie.

Funding This study was supported by the University of Ferrara through the Futuro In Ricerca grant (FIR-2018 granted to SP) and the Fondo di Ateneo per la Ricerca Scientifica (FAR granted to SP and CB).

Data availability The datasets generated during and/or analysed during the current study are available from the corresponding author on reasonable request.

Declarations

Conflict of interest The authors declare no competing interests.

References

Abo-Shady AM, Mohamed YA, Lasheen T (1993) Chemical composition of the cell wall in some green algae species. Biol Plant 35:629–632

Albanese P, Nield J, Tabares JAM, Chiodoni A, Manfredi M, Gosetti F (2016) Isolation of novel PSII-LHCII megacomplexes from pea plants characterized by a combination of proteomics and electron microscopy. Photosynth Res 1-13

Ambati RR, Gogisetty D, Aswathanarayana RG, Ravi S, Bikkina PN, Bo L, Yuepeng S (2019) Industrial potential of carotenoid pigments from microalgae: current trends and future prospects. Crit Rev Food Sci Nutr 59:1880–1902

Amorim ML, Soares J, dos Reis Coimbra JS, de Oliveira LM, Teixeira Albino LF (2021) Microalgae proteins: production, separation, isolation, quantification, and application in food and feed. Crit Rev Food Sci Nutr 61:1976–2002

Anderson JM, Chow WS, Park YI (1995) The grand design of photosynthesis: acclimation of the photosynthetic apparatus to environmental cues. Photosynth Res 46:129–139

Baldisserotto C, Giovanardi M, Ferroni L, Pancaldi S (2014) Growth, morphology and photosynthetic responses of *Neochloris oleoabundans* during cultivation in a mixotrophic brackish medium and subsequent starvation. Acta Physiol Plant 36:461–472

Baldisserotto C, Popovich C, Giovanardi M, Sabia A, Ferroni L, Constenla D, Leonardi P, Pancaldi S (2016) Photosynthetic aspects and lipid profiles in the mixotrophic alga *Neochloris oleoabundans* as useful parameters for biodiesel production. Algal Res 16:1

Baldisserotto C, Demaria S, Accoto O, Marchesini R, Zanella M, Benetti L et al (2020) Removal of nitrogen and phosphorus from thickening effluent of an urban wastewater treatment plant by an isolated green microalga. Plants 9:1802

Barbarino E, Lourenço SO (2005) An evaluation of methods for extraction and quantification of protein from marine macro- and microalgae. J Appl Phycol 17:447–460

Barka A, Blecker C (2016) Microalgae as a potential source of single-cell proteins. A review. Biotechnol Agron Soc Environ 20:427–436

Bennett J (1991) Protein phosphorylation in green plant chloroplasts. Annu Rev Plant Biol 42:281–311

Bielczynski LW, Schansker G, Croce R (2016) Effect of light acclimation on the organization of photosystem II super-and sub-complexes in *Arabidopsis thaliana*. Front Plant Sci 7:105

Büchel C (2015) Evolution and function of light harvesting proteins. J Plant Physiol 172:62–75

Buono S, Langellotti AL, Martello A, Rinna F, Fogliano V (2014) Functional Ingredients from Microalgae. Food Funct 5:1669–1685

Calvaruso C, Rokka A, Aro E-M, Büchel C (2020) Specific Lhc proteins are bound to PSI or PSII supercomplexes in the diatom *Thalassiosira pseudonana*. Plant Physiol 183:67–79

Camacho F, Macedo A, Malcata F (2019) Potential industrial applications and commercialization of microalgae in the functional food and feed industries: a short review. Mar Drugs 17:312

Chacón-Lee TL, González-Mariño GE (2010) Microalgae for "healthy" foods—possibilities and challenges. Compr Rev Food Sci Food Saf 9:655–675

Chantanachat S, Bold HC (1962) Phycological studies. II. Some algae from arid soils. Univ Tex Publ 6218:1–74

Chevallet M, Luche S, Rabilloud T (2006) Silver staining of proteins in polyacrylamide gels. Nat Protoc 1:1852–1858

Crepin A, Caffarri S (2018) Functions and evolution of Lhcb isoforms composing LHCII, the major light harvesting complex of photosystem II of green eukaryotic organisms. Curr Protein Pept Sci 19:699–713

da Silva MET, de Paula CK, Martins MA, da Matta SLP, Martino HSD, dos Reis Coimbra JS (2020) Food safety, hypolipidemic and hypoglycemic activities, and in vivo protein quality of microalga *Scenedesmus obliquus* in Wistar rats. J Funct Foods 65:103711

Damiani MC, Popovich CA, Constenla D, Martínez AM, Doria E, Longoni P, Cella R, Nielsen E, Leonardi PI (2014) Triacylglycerol content, productivity and fatty acid profile in *Scenedesmus acutus* PVUW12. J Appl Phycol 26:1423–1430

Deblois CP, Marchand A, Juneau P (2013) Comparison of photoacclimation in twelve freshwater photoautotrophs (Chlorophyte, Bacillaryophyte, Cryptophyte and Cyanophyte) isolated from a natural community. PLoS ONE 8:e57139

Dekker JP, Boekema EJ (2005) Supramolecular organization of thylakoid membrane proteins in green plants. Biochim Biophys Acta Bioenerget 1706:12–39

Devadsu E, Pandey J, Dhokne K, Subramanyam R (2021) Restoration of photosynthetic activity and supercomplexes from severe iron starvation in *Chlamydomonas reinhardtii*. Biochim Biophys Acta Bioenerget 1862:148331

Di Stefano E, Agyei D, Njoku EN, Udenigwe CC (2018) Plant PuBisCo: and underutilized protein for food applications. J Am Oil Chem Soc 95:1063–1074

Difusa A, Talukdar J, Kalita MC, Mohanty K, Goud VV (2015) Effect of light intensity and pH condition on the growth, biomass and lipid content of microalgae *Scenedesmus* species. Biofuels 6:37–44

Dixon C, Wilken LR (2018) Green microalgae biomolecule separations and recovery. Bioresour Bioprocess 5:14

Durnford DG, Price JA, McKim SM, Sarchfield ML (2003) Light-harvesting complex gene expression is controlled by both transcriptional and post-transcriptional mechanisms during photoacclimation in *Chlamydomonas reinhardtii*. Physiol Plant 118:193–205

Falkowski PG (1980) Light-shade adaptation in marine phytoplankton. In: Falkowski PG (ed) Primary Productivity in the Sea. Springer, Boston pp 99–119

Fang L, Leliaert F, Zhang ZH, Penny D, Zhong BJ (2017) Evolution of the Chlorophyta: insights from chloroplast phylogenomic analyses. J Syst Evol 55:322–332

FAO (2020) Food outlook - biannual report on global food markets: 2020. Food Outlook, 1. Rome.

Ferroni L, Angeleri M, Pantaleoni L, Pagliano C, Longoni P, Marsano F et al (2014) Light-dependent reversible phosphorylation of the minor photosystem II antenna Lhcb6 (CP24) occurs in lycophytes. Plant J 77:893–905

Ferroni L, Suorsa M, Aro E-M, Baldisserotto C, Pancaldi S (2016) Light acclimation in the lycophyte *Selaginella martensii* depends on changes in the amount of photosystems and on the flexibility of the light-harvesting complex II antenna association with both photosystems. New Phytol 211:554–568

Ferroni L, Cucuzza S, Angeleri M, Aro EM, Pagliano C, Giovanardi M et al (2018) In the lycophyte *Selaginella martensii* is the "extra-qT" related to energy spillover? Insights into photoprotection in ancestral vascular plants. Environ Exp Bot 154:110–122

Finazzi G, Minagawa J (2014) High light acclimation in green microalgae. In: Demmig-Adams B, Garab G, Adams III W, Govindjee (eds). Non-photochemical quenching and energy dissipation in plants, algae and cyanobacteria. Springer, Dordrecht, pp. 445–469

Furukawa R, Aso M, Fujita T, Akimoto S, Tanaka R, Tanaka A, Yokono M, Takabayashi A (2019) Formation of a PSI-PSII megacomplex containing LHCSR and PsbS in the moss *Physcomitrella patens*. J Plant Res 132:867–880

Galka P, Santabarbara S, Khuong TTH, Degand H, Morsomme P, Jennings RJ, Boekema EJ, Caffarri S (2012) Functional analyses of the plant photosystem I-light-harvesting complex II supercomplex reveal that light-harvesting complex II loosely bound to photosysmtem II is a very efficient antenna for photosystem I in state II. Plant Cell 24:2963–2978

Gao C, Wang Y, Shen Y, Yan D, He X, Dai J, Wu Q (2014) Oil accumulation mechanisms of the oleaginous microalga *Chlorella protothecoides* revealed through its genome, transcriptomes, and proteomes. BMC Genomics 15:1

Garcìa-Cerdàn JG, Furst AL, McDonald KL, Schünemann S, Francis MB, Nyiogi KK (2019) A thylakoid membrane-bound and redox-active rubredoxin (RBD1) functions in de novo assembly and repair of photosystem II. Proc Natl Acad Sci 116:16631–16640

Garrido-Cardenas JA, Manzano-Agugliaro F, Acien-Fernandez F, Molina Grima E (2018) Microalgae research worldwide. Algal Res 35:50–60

Giovanardi M, Ferroni L, Baldisserotto C, Tedeschi P, Maietti A, Pantaleoni L, Pancaldi S (2013) Morpho-physiological analyses of

Neochloris oleoabundans (Chlorophyta) grown mixotrophically in a carbon-rich waste product. Protoplasma 250:161–174

Giovanardi M, Poggioli M, Ferroni L, Lespinasse M, Baldisserotto C, Aro EM, Pancaldi S (2017) Higher packing of thylakoid complexes ensures a preserved photosystem II activity in mixotrophic *Neochloris oleoabundans*. Algal Res 25:322–332

Giovanardi M, Pantaleoni L, Ferroni L, Pagliano C, Albanese P, Baldisserotto C, Pancaldi S (2018) In pea stipules a functional photosynthetic electron flow occurs despite a reduced dynamicity of LHCII association with photosystems. Biochim Biophys Acta Bioenerg 1859:1025–1038

Grieco M, Suorsa M, Jajoo A, Tikkanen M, Aro E-M (2015) Light-harvesting II antenna trimers connect energetically the entire photosynthetic machinery – including both photosystems II and I. Biochim Biophys Acta 1847:607–619

Griffiths MJ, Garcin C, van Hille RP, Harrison ST (2011) Interference by pigment in the estimation of microalgal biomass concentration by optical density. J Microbiol Methods 85:119–123

Havlik I, Lindner P, Schepe T, Reardon KF (2013) On-line monitoring of large cultivations of microalgae and cyanobacteria. Trends Biotechnol 31:406–414

Hayes M, Skomedal H, Skjånes K, Mazur-Marzec H, Torùnska-Sitarz A, Catala M, Isleten Hosoglu M, García-Vaquero M (2017) Microalgal proteins for feed, food and health. In: Gonzalez-Fernandez C, Muñoz R (eds) Microalgae-based biofuels and bioproducts: from feedstock cultivation to end-products. Elsevier-Woodhead Publishing, Duxford pp 347–368

Henchion M, Hayes M, Mullen AM, Fenelon M, Tiwari B (2017) Future protein supply and demand: strategies and factors influencing a sustainable equilibrium. Foods 6:53

Heredia-Arroyo T, Wei W, Hu B (2010) Oil accumulation via heterotrophic/mixotrophic *Chlorella protothecoides*. Appl Biochem Biotechnol 162:1978–1995

Humby PL, Durnford DG (2006) Photoacclimation: physiological and molecular responses to changes in light environments. In: Huang B (ed) Plant–environment interactions. CRC Press, Boca Raton, pp 69–99

Ivleva NB, Golden SS (2007) Protein extraction, fractionation, and purification from Cyanobacteria. In: Rosato E (eds), Circadian rhythms, Methods in molecular biology, Humana Press, Totowa pp 365–373

Jayappriyan KR, Baskar B, Vijayakumar M, Brabakaran A, Rajkumar R, Elumalai S (2021) Food and nutraceutical applications of algae. In: Raja R, Hemaiswarya S, Arunkumar K, Carvalho IS (Eds) Algae for food. CRC Press, Boca Raton

Järvi S, Suorsa M, Paakkarinen V, Aro E-M (2011) Optimized native gel systems for separation of thylakoid protein complexes: novel super- and mega-complexes. Biochem J 439:207–214

Kalaji HM, Schansker G, Ladle RJ, Vasilij Goltsev V, Bosa K, Allakhverdiev SI et al (2014) Frequently asked questions about in vivo chlorophyll fluorescence: practical issues. Photosynth Res 122:121–158

Kantzilakis K, Aivaliotis M, Kotakis C, Krasanakis F, Rizos AK, Kotzabasis K, Tsiotis G (2007) A comparative approach towards thylakoid membrane proteome analysis of unicellular green alga *Scenedesmus obliquus*. Biochim Biophys Acta Biomembr 1768:2271–2279

Khalil ZI, Asker MM, El-Sayed S, Kobbia IA (2010) Effect of pH on growth and biochemical responses of *Dunaliella bardawil* and *Chlorella ellipsoidea*. World J Microbiol Biotech 26:1225–1231

Khan MI, Shin JH, Kim JD (2018) The promising future of microalgae: current status, challenges, and optimization of a sustainable and renewable industry for biofuels, feed, and other products. Microb Cell Fact 17:36

Kouřil R, Dekker JP, Boekema EJ (2012) Supramolecular organization of photosystem II in green plants. Biochim Biophys Acta Bioenerget 1817:2–12

Krienitz L, Huss VA, Bock C (2015) *Chlorella*: 125 years of the green survivalist. Trends Plant Sci 20:67–69

Kubota-Kawai H, Burton-Smith RN, Tokutsu R, Song C, Akimoto S, Yokono M, Ueno Y, Kim E, Watanabe A, Murata K, Minagawa J (2019) Ten antenna proteins are associated with the core in the supramolecular organization of the photosystem I supercomplex in *Chlamydomonas reinhardtii*. J Biol Chem 294:4304–4314

Kügler M, Jänsch L, Kruft V, Schmitz UK, Braun HP (1997) Analysis of the chloroplast protein complexes by blue-native polyacrylamide gel electrophoresis (BN-PAGE). Photosynth Res 53:35–44

Laemmli U (1970) Cleavage of structural proteins during the assembly of the head of bacteriophage T4. Nature 227:680–685

Laurens LM, Van Wychen S, McAllister JP, Arrowsmith S, Dempster TA, McGowen J et al (2014) Strain, biochemistry, and cultivation-dependent measurement variability of algal biomass composition. Anal Biochem 452:86–95

Leliaert F, Smith DR, Moreau H, Herron MD, Verbruggen H, Delwiche CF, De Clerck O (2012) Phylogeny and molecular evolution of the green algae. Crit Rev Plant Sci 31:1–46

Li Y, Wang C, Liu H, Su J, Lan CQ, Zhong M, Hu X (2020) Production, isolation and bioactive estimation of extracellular polysaccharides of green microalga *Neochloris oleoabundans*. Algal Res 48:101883

Lichtenthaler HK, Buschmann C, Knapp M (2005) How to correctly determine the different chlorophyll fluorescence parameters and the chlorophyll fluorescence decrease ratio RFd of leaves with the PAM fluorometer. Photosynthetica 43:379–393

Lourenço SO, Barbarino E, Lavín PL, Marquez UML, Aidar E (2004) Distribution of intracellular nitrogen in marine microalgae: calculation of new nitrogen-to-protein conversion factors. Eur J Phycol 39:17–32

Maglie M, Baldisserotto C, Guerrini A, Sabia A, Ferroni L, Pancaldi S (2021) A co-cultivation process of *Nannochloropsis oculata* and *Tisochrysis lutea* induces morpho-physiological and biochemical variations potentially useful for biotechnological purposes. J Appl Phycol 33:2817–2832

Markwell MAK, Haas SM, Tolbert NE, Bieber LL (1981) Protein determination in membrane and lipoprotein samples: manual and automated procedures. Methods Enzymol 72:296–303

Meijer EA, Wijffels RH (1998) Development of a fast, reproducible and effective method for the extraction and quantification of proteins of micro-algae. Biotechnol Tech 12:353–358

Mettler T, Mühlhaus T, Hemme D, Schöttler MA, Rupprecht J, Idoine A et al (2014) Systems analysis of the response of photosynthesis, metabolism, and growth to an increase in irradiance in the photosynthetic model organism *Chlamydomonas reinhardtii*. Plant Cell 26:2310–2350

Minagawa J, Takahashi Y (2004) Structure, function and assembly of photosystem II and its light-harvesting proteins. Photosynth Res 8:241–263

Moheimani NR (2013) Inorganic carbon and pH effect on growth and lipid productivity of *Tetraselmis suecica* and *Chlorella* sp. (Chlorophyta) grown outdoors in bag photobioreactors. J Appl Phycol 25:387–398

Nama S, Madireddi SK, Devadasu ER, Subramanyam R (2015) High light induced changes in organization, protein profile and function of photosynthetic machinery in *Chlamydomonas reinhardtii*. J Photochem Photobiol B 152:367–376

Nama S, Madireddi SK, Yadav RM, Subramanyam R (2019) Non-photochemical quenching-dependent acclimation and thylakoid organization of *Chlamydomonas reinhardtii* to high light stress. Photosynth Res 139:387–400

Nelson N, Ben-Shem A (2004) The complex architecture of oxygenic photosynthesis. Nat Rev Mol Cell Biol 5:971–982

Parisi G, Tulli F, Fortina R, Marino R, Bani P, Dalle Zotte A et al (2020) Protein hunger of the feed sector: the alternatives offered by the plant world. Ital J Anim Sci 19:1204–1225

Park H, Eggink LL, Roberson RW, Hoober JK (1999) Transfer of proteins from the chloroplast to vacuoles in *Chlamydomonas reinhardtii* (Chlorophyta): a pathway for degradation. J Phycol 35:528–538

Patel A, Matsakas L, Rova U, Christakopoulos P (2018) Heterotrophic cultivation of *Auxenochlorella protothecoides* using forest biomass as a feedstock for sustainable biodiesel production. Biotechnol Biofuels 11:169

Patnaik R, Mallick N (2015) Utilization of *Scenedesmus obliquus* biomass as feedstock for biodiesel and other industrially important co-products: an integrated paradigm for microalgal biorefinery. Algal Res 12:328–336

Popovich CA, Damiani MC, Constenla D, Martínez AM, Freije H, Giovanardi M, Pancaldi S, Leonardi PI (2012) *Neochloris oleoabundans* grown in natural enriched seawater for biodiesel feedstock: evaluation of its growth and biochemical composition. Bioresour Technol 114:287–293

Porra RJ, Thompson WA, Kriedemann PE (1989) Determination of accurate extinction coefficients and simultaneous-equations for assaying chlorophyll-*a* and chlorophyll-*b* extracted with 4 different solvents: verification of the concentration of chlorophyll standards by atomic-absorption spectroscopy. Biochim Biophys Acta 975:384–394

Pruvost J, Van Vooren G, Cogne G, Legrand J (2009) Investigation of biomass and lipids production with *Neochloris oleoabundans* in photobioreactor. Bioresour Technol 100:5988–5995

Pruvost J, Van Vooren G, Le Gouic B, Couzinet-Mossion A, Legrand J (2011) Systematic investigation of biomass and lipid productivity by microalgae in photobioreactors for biodiesel application. Bioresour Technol 102:150–158

Rashidi B, Trinidade LM (2018) Detailed biochemical and morphologic characteristics of the green microalga *Neochloris oleoabundans* cell wall. Algal Res 35:152–159

Rokka A, Suorsa M, Saleem A, Battchikova N, Aro EM (2005) Synthesis and assembly of thylakoid protein complexes: multiple assembly steps of photosystem II. Biochem J 388:159–168

Sabia A, Baldisserotto C, Biondi S, Marchesini R, Tedeschi P, Maietti A, Giovanardi FL, Pancaldi S (2015) Re-cultivation of *Neochloris oleoabundans* in exhausted autotrophic and mixotrophic media: the potential role of polyamines and free fatty acids. Appl Microbiol Biotechnol 99:10597–10609

Safi C, Charton M, Pignolet O, Silvestre F, Vaca-Garcia C, Pontalier PY (2013) Influence of microalgae cell wall characteristics on protein extractability and determination of nitrogen-to-protein conversion factors. J Appl Phycol 25:523–529

Schuurmans RM, van Alphen P, Schuurmans JM, Matthijs HC, Hellingwerf KJ (2015) Comparison of the photosynthetic yield of cyanobacteria and green algae: different methods give different answers. PLoS ONE 10:e0139061

Serive B, Kaas R, Bérard JB, Pasquet V, Picot L, Cadoret JP (2012) Selection and optimisation of a method for efficient metabolites extraction from microalgae. Bioresour Technol 124:311–320

Singh SP, Singh P (2015) Effect of temperature and light on the growth of algae species: a review. Renew Sust Energ Rev 50:431–444

Spain O, Plöhn M, Funk C (2021) The cell wall of green microalgae and its role in heavy metal removal. Physiol Plant 173:526–535

Spolaore P, Joannis-Cassan C, Duran E, Isambert A (2006) Commercial applications of microalgae. J Biosci Bioeng 101:87–96

Spreitzer RJ (1993) Genetic dissection of Rubisco structure and function. Annu Rev Plant Biol 44:411–434

Stankovic B (2018) Plants in space. In: Russomano T, Rehnberg L (eds) Into space - a journey of how humans adapt and live in microgravity, IntechOpen, Riejeka pp 153–170

Szyszka-Mroz B, Pittock P, Ivanov AG, Lajoie G, Hüner NP (2015) The Antarctic psychrophile, *Chlamydomonas* sp. UWO 241, preferentially phosphorylates a PSI-cytochrome b_6f supercomplex. Plant Physiol 169:717-736

Torres-Tiji Y, Fields FJ, Mayfield SP (2020) Microalgae as a future food source. Biotechnol Adv 41:107536

Tran NP, Park JK, Lee CG (2009) Proteomics analysis of proteins in green alga *Haematococcus lacustris* (Chlorophyceae) expressed under combined stress of nitrogen starvation and high irradiance. Enzyme Microb Tech 45:241–246

Umetani I, Kunugi M, Yokono M, Takabayashi A, Tanaka A (2018) Evidence of the supercomplex organization of photosystem II and light-harvesting complexes in *Nannochloropsis granulata*. Photosynth Res 136:49–61

Ursu AV, Marcati A, Sayd T, Sante-Lhoutellier V, Djelveh G, Michaud P (2014) Extraction, fractionation and functional properties of proteins from the microalgae *Chlorella vulgaris*. Bioresour Technol 157:134–139

van den Berg TE, Arshad R, Nawrocki WJ, Boekema EJ, Kouřil CR (2020) PSI of the colonial alga *Botryococcus braunii* has an unusually large antenna size. Plant Physiol 184:2014–2051

Villarejo A, Orus MI, Martinez F (1995) Coordination of photosynthetic and respiratory metabolism in *Chlorella vulgaris* UAM-101 in the light. Physiol Plant 94:680–686

Voigt J, Stolarczyk A, Zych M, Malec P, Burczyk J (2014) The cell-wall glycoproteins of the green alga *Scenedesmus obliquus*. The predominant cell-wall polypeptide of *Scenedesmus obliquus* is related to the cell-wall glycoprotein gp3 of *Chlamydomonas reinhardtii*. Plant Sci 215–216:39–47

Wellburn AR (1994) The spectral determination of chlorophylls a and b, as well as total carotenoids, using various solvents with spectrophotometer of different resolution. J Plant Physiol 144:307–313

Wells ML, Potin P, Craigie JS, Raven JA, Merchant SS, Helliwell KE, Smith AG, Camire ME, Brawley SH (2017) Algae as nutritional and functional food sources: revisiting our understanding. J Appl Phycol 29:949–982

White S, Anandraj A, Bux F (2011) PAM fluorometry as a tool to assess microalgal nutrient stress and monitor cellular neutral lipids. Bioresour Technol 102:1675–1682

Wobbe L, Bassi R, Kruse O (2016) Multi-level light capture control in plants and green algae. Trends Plant Sci 21:55–68

Wu C, Xiong W, Dai J, Wu Q (2015) Genome-based metabolic mapping and ^{13}C flux analysis reveal systematic properties of an oleaginous microalga *Chlorella protothecoides*. Plant Physiol 167:586–599

Yokono M, Takabayashi A, Akimoto S, Tanaka A (2015) A megacomplex composed of both photosystem reaction centres in higher plants. Nature Comm 6:6675

Yokono M, Takabayashi A, Kishimoto J, Fujita T, Iwai M, Murakami A, Akimoto S, Tanaka A (2019) The PSI-PSII megacomplex in green plants. Plant Cell Physiol 60:1098–1108

Zerveas S, Mente MS, Tsakiri D, Kotzabasis K (2021) Microalgal photosynthesis induces alkalization of aquatic environment as a result of H^+ uptake independently from CO_2 concentration – new perspectives for environmental applications. J Environ Manage 289:112546

Zhao L, Cheng D, Huang X, Chen M, Dall'Osto L, Xing J, Gao L, Li L, Wang Y, Bassi R, Peng L, Wang Y, Rochaix J-D, Huang F (2017) A light harvesting complex-like protein in maintenance of photosynthetic components in *Chlamydomonas*. Plant Physiol 174:2419–2433